**Title of manuscript**

Auger electron spectroscopic analysis of corrosion products formed on A3003 aluminum alloy in model fresh water with different $Zn^{2+}$ concentration

**Author Names**

Kyohei Otani[1, 2)], Md. Saiful Islam[1)], Masatoshi Sakairi[3)], and Akira Kaneko[4)]

**Affiliations**

1) Graduate School of Engineering, Hokkaido University, Japan

2) Sector of Nuclear Science Research, Japan Atomic Energy Agency

3) Faculty of Engineering, Hokkaido University, Japan

4) Nikkei Research & Development Center, Nippon Light Metal co. Ltd., Japan

**Corresponding Author, E-mail:**

msakairi@eng.hokuda.ac.jp

**Abstract**

The corrosion morphology and composition of corrosion products of A3003 formed in model fresh water with different $Zn^{2+}$ concentrations were investigated by immersion tests combined with surface observations and analysis using an auger electron spectroscope (AES). The cross-sectional AES observations showed that the thickness of the corrosion product layer formed on A3003 decreases with increases in the $Zn^{2+}$ concentration of the model fresh water. A cross-sectional AES point analysis suggested that the corrosion products formed on the A3003 in the $Zn^{2+}$ containing model fresh water ($Zn^{2+}$ > 0.1 mM) have a multi-layer structure, and that the inner of Zn rich layer would have high corrosion protective properties.

**Keywords**: corrosion, aluminum alloy, oxide film, metal cation, fresh water

## Introduction

Aluminum alloys are widely used in many environments because of the good corrosion resistance and high strength/weight ratio. The protective films on the alloys are essential factor in the high corrosion resistance. The protective films are easily destroyed by $Cl^-$ in solution, and the corrosion rate of aluminum alloys depends on the concentration of $Cl^-$ in the solutions.[1-3] The corrosion rate of aluminum alloys changes in fresh water sampled in different locations despite similar $Cl^-$ concentrations.[4] Fresh water also contains dilute metal cations, however, there have been few studies focusing on the effects of metal cations on the corrosion behavior of aluminum alloys in tap water.[5,6] For this reason, the authors expected that the metal cations would change the corrosion rate of aluminum alloys in fresh waters.

The authors have been investigating the corrosion of aluminum alloys in fresh water focused on the effects of metal cations.[7-10] This research has focused on the effects of metal cations, and showed that the corrosion rate of A3003 aluminum alloy in fresh water is changed by the kinds of metal cations in the model fresh water where the concentration of $Cl^-$, dissolved oxygen, and pH are similar. This research also established that $Zn^{2+}$ is superior to inhibit the fresh water corrosion of A3003 among the metal cations used in the studies.[9,10] However, the minimum concentration of $Zn^{2+}$ to inhibit the corrosion of A3003 in model fresh water has not been determined. Establishing the minimum concentration of metal cations is important to be able to use the metal cations in industrial environments as corrosion inhibitors. In addition, the morphology of corrosion products formed on A3003 in model fresh water containing $Zn^{2+}$ and the corrosion inhibition mechanism by $Zn^{2+}$ also have not been established.

In the present research, the corrosion behaviors and the corrosion products of A3003 formed in fresh water with different $Zn^{2+}$ concentrations were investigated by immersion tests combined with surface observation and an analysis using auger electron spectroscope (AES).

The high-resolution analysis by AES (maximum resolution 8 nm) will contribute to understand the structure of corrosion products formed on A3003 after immersion tests. The aim of this study is to determine the minimum concentration of $Zn^{2+}$ which inhibits the corrosion of A3003 aluminum alloy in model fresh water, and to establish the details of the corrosion inhibition mechanism for the aluminum alloy in model fresh water containing $Zn^{2+}$ by surface observations and analysis.

## Experimental

### Specimens

The specimens were A3003-H24 sheets (composition (mass%): Cu, 0.11; Si, 0.36; Fe, 0.55; Mn, 1.08; Mg, <0.01; Zn, 0.01; Ti, 0.03, Al: bal.), cut into a size of 7 × 7 × 1.0 mm. The specimens were embedded in epoxy resin (Struers Ltd., EpoFix Resin). The exposed surfaces of the embedded specimens were ground with SiC abrasive paper from #600 to #4000 grit size and finally polished by buffing. Before the tests, specimens were taken out from the resin and ultrasonically cleaned in ethanol and then in highly purified water.

### Solutions and immersion tests

The following four solutions with different $Zn^{2+}$ concentrations, 2.0 mM NaCl (NaCl), 0.01 mM $ZnCl_2$ + 1.98 mM NaCl (0.01Zn), 0.1 mM $ZnCl_2$ + 1.8 mM NaCl (0.1Zn), and 1 mM $ZnCl_2$ (1.0Zn) were used as test solutions. The concentration of $Cl^-$ in the solutions was adjusted to 2.0 mM and the pH of the solutions were approximately 6. All chemicals were special grade and obtained from Kanto Chemical Co., Ltd. Specimens were immersed in the solutions for 7 d (0.6 Ms) at 298 K in bottles, with the bottles open to the air during the immersion tests. The surfaces and cross-section of the specimens were observed by an auger electron spectroscope (AES, JEOL Ltd., JAMP-9500 F). The specimen morphology was observed by the scanning

electron microscope (SEM) function of the AES. A cross-section polisher (CP, JEOL Ltd., SM-09010) was used to prepare cross-sections of the specimens. The cross-sectional structures of the immersed specimens were also analyzed by the AES. An Ar ion sputtering gun was used to clean contamination form the specimens.

## Results and discussion

### Surface and cross-sectional morphology of specimens before the immersion tests

Fig. 1 shows (a) surface and (b) cross-sectional SEM images of specimens before the immersion tests. There are white and black particles and gray aluminum matrix at the surface of the specimen (Fig. 1 (a)). In a previous study,[11] the white particles were identified as Al-Mn-Fe intermetallic compounds and the black particles were Al-Si intermetallic compounds. The cross-sectional SEM image shows that the surface of the specimens before the immersion tests is perfectly flat (Fig. 1 (b)). A conductive resin containing Ag particles were used for the cross-sectional observations in this study, and white Ag particles and black resin region are shown in the cross-sectional image.

### Surface observations and analysis

Fig. 2 shows surface SEM images of specimens after immersion for 7 d in (a) NaCl, (b) 0.01Zn, (c) 0.1Zn, and (d) 1.0Zn. A smooth surface and some protuberances are observed on the specimen after immersion in NaCl, and a smooth surface and dome-shaped sites are observed on the specimen after immersion in 0.01Zn and 0.1Zn (Fig. 2 (a), (b), and (c)). There is a rough surface and dome-shaped sites on the specimen after immersion in 1.0Zn (Fig. 2 (d)). The surface SEM images show that significant amount of corrosion products are formed on the 1.0 Zn specimen more than on the other specimens. There are no intermetallic compounds on any of the specimens like those which were observed on the specimens before the immersion

tests in Fig. 1 (a). This means that the thick corrosion products were formed on the specimens in all the solutions and then the metallic surface of the aluminum alloy is covered by corrosion products.

Fig. 3 shows the surface AES point analysis of the specimens after immersion in the solutions for 7 d, and the analytical points are those indicated (+) in Fig. 2. From the AES analysis, the composition of the flat and the dome-shaped areas are very similar. The AES spectra of all the specimens show O and Al peaks, and the spectra of the specimens immersed in 0.1Zn and 1.0Zn show Zn peaks. This result indicates that Al corrosion products were formed on the specimen in NaCl and 0.01Zn, and that Al/Zn corrosion products were formed on the specimen immersed in 0.1Zn and 1.0Zn.

**Cross-sectional observations and analysis**

Cross-sectional observations and analysis were carried out to establish the cross-sectional structure of the specimens after the corrosion experiments. Cross-sectional SEM images of specimens after immersion for 7 d in (a) NaCl, (b) 0.01Zn, (c) 0.1Zn, and (d) 1.0Zn are shown in Fig. 4. A cross-sectional SEM image after immersion in NaCl (Fig. 4 (a)) shows that the thickness of the corrosion product layer formed on a non-pit region is approximately 1 μm, and that dome-shaped corrosion products are formed on the large pits (Fig. 4(a)). Large pits are also observed under the dome-shaped corrosion products in the specimen immersed in 0.01Zn, and the thickness of the corrosion product layer formed on a non-pit region is similar to that of the specimen immersed in NaCl (Fig. 4(b)). The cross-sectional SEM image of the 0.01Zn specimen indicates that the dome-shaped corrosion products which were observed in Fig. 3 form on the large pits sites. The dome-shaped corrosion products on the large pits and a thin corrosion product layer (less than 100 nm) can be seen in the specimen immersed in 0.1Zn (Fig. 4(c)). The corrosion products on the large pits formed in 0.1Zn are composed of white and gray

regions, and this indicates that the corrosion products would be of a multi-layer structure. A small pit and dome-shaped products are observed in the SEM image of the 1.0Zn specimen, and here it is difficult to identify a corrosion product layer (Fig. 4 (d)). The cross-sectional SEM image of 1.0Zn indicates that the dome-shaped products formed in the 1.0Zn experiment also have a multi-layer structure, and that products are not formed on the pit site. These cross-sectional observations suggest that 1.0 mM Zn ions in fresh water can prevent formation of large pits in the A3003 alloys, and that the thickness of the corrosion product layer decreases with increases of $Zn^{2+}$ concentration in the model fresh water here.

The results of the cross-sectional AES point analysis of the specimens after immersion in solutions for 7 d are shown in Fig. 5. Three or four different positions were analyzed on each specimen and the analytical positions are indicated (+) in Fig. 4. The AES spectra of the corrosion products formed on the specimens immersed in NaCl and 0.01Zn have O and Al peaks, indicating that aluminum carbonate or hydroxides are formed on the specimen in NaCl and 0.01Zn (Fig. 5 (a) and (b)). These results show that the corrosion products formed in NaCl and in 0.01Zn are without corrosion protective properties. Zinc peaks are detected in the corrosion products formed on the pits of the specimen immersed in 0.1Zn, and the zinc peak heights of the white region is larger than that of the gray region in Fig. 4(c) (Fig. 5 (c)). This indicates that the multi-layer corrosion products are composed of a zinc rich layer (inner white layer) and an aluminum rich layer (outer gray layer). Zinc peaks are also detected in the corrosion products on the specimen immersed in 1.0Zn (Fig. 5 (d)), and the zinc peak heights obtained from the white zinc rich layer is larger than that obtained with 0.1Zn. This means that the zinc rich layer formed in 1.0Zn contains more $Zn^{2+}$ than the layer formed in 0.1Zn, and that the zinc rich layer formed on the specimen has very good corrosion protective properties for the A3003 alloy in fresh water. The results of this study indicate that the minimum concentration of $Zn^{2+}$ which can inhibit corrosion of A3003 in model fresh water would be 0.1

mM.

**Formation and corrosion protection mechanism of metal cation layer of $Zn^{2+}$**

The formation and corrosion protection mechanism of the metal cation layer of $Zn^{2+}$ is detailed in Fig. 6 (a) and (b). Several studies have reported that an $Al_2O_3$ layer (5-10 nm thickness) is formed on aluminum alloys[10, 12], and that the layer has $OH^-$ sites at the solution/$Al_2O_3$ interface[13,14]. Hard and soft acids and bases (HSAB) theory has reported that hard acids and hard bases form strong bonds[15, 16]. Commonly, $Zn^{2+}$ is categorized as a hard acid and $OH^-$ as a hard base, from this it may be proposed that $Zn^{2+}$ easily bonds with the $OH^-$ on the $Al_2O_3$ layer on aluminum alloys (Fig. 6 (a)). Our previous study established that a metal cation layer of $Zn^{2+}$ (10-15 nm thickness) was formed on $Al_2O_3$ in model fresh water containing $Zn^{2+}$, and that the metal cation layer had high corrosion protective properties (Fig. 6 (b)) [10]. In the previous study,[9] the polarization curve for A3003 aluminum alloy obtained in model fresh water containing $Zn^{2+}$ suggested that the metal cation layer of $Zn^{2+}$ on the aluminum alloy suppresses both the anodic (metal oxidation) and cathodic (oxygen reduction) reactions. This means that the layer of $Zn^{2+}$ on the aluminum alloy would prevent the $Cl^-$ form any attack and also the oxygen diffusion to the metal and oxide film interface. It is considered that the suppression of activity is the main factor giving the metal cation layer of $Zn^{2+}$ strong corrosion protective properties. Some studies[17-19] reported that coverage of the protective film formed on metals by chemical bonding depends on the concentration of ions in the surrounding solutions. This would suggest that the metal cation layer formed at the low $Zn^{2+}$ concentration has many defects (no covered sites), and that the number of defects in the protective metal cation layer would depend on the $Zn^{2+}$ concentration of the model fresh water. This is a possible reason why the thickness of the corrosion product layer decreased with increases in the $Zn^{2+}$ concentration of the model fresh waters as shown in Fig. 4.

## Formation and corrosion protection mechanism of corrosion products containing $Zn^{2+}$

The formation and corrosion protection mechanism of Zn/Al corrosion products are explained in Figs. 6 (c) and (d). After long term immersion in the model fresh water, the corrosion process of the aluminum alloy changes to a coupled electrochemical reaction consisting of anodic metal oxidation at the defects (1) and cathodic oxygen reduction (2):

$$Al \rightarrow Al^{3+} + 3e^- \quad (1)$$

$$1/2O_2 + H_2O + 2e^- \rightarrow 2OH^- \quad (2)$$

The cathodic reaction would occur at the deposited intermetallic compound because the intermetallic compound formation on the specimen is more novel than the aluminum matrix. A result of this would be that the pH of the model fresh water near the intermetallic compound would be increased by the cathodic reaction, and that the increase in pH would lead to the formation of hydroxides of Al and Zn on the intermetallic compound (Fig. 6 (c)). The AES observations and analysis in this study showed that the thickness of the corrosion products is 100-1000 nm, and the corrosion products containing high concentrations of $Zn^{2+}$ have good corrosion protective properties (Fig. 6 (d)). Aramaki[20] reported that zinc corrosion products inhibit cathodic reactions on the metal and prevents oxygen diffusion from the solution to the metal surface. This suggests that the Zn/Al corrosion products (Zn rich) would act to inhibit the cathodic reactions which occur on the intermetallic compounds. The cross-sectional AES analyses in this study showed that the Zn/Al corrosion products were detected only in the specimens immersed in the model fresh water containing more than 0.1 mM of $Zn^{2+}$. Therefore, it can be posited that the minimum concentration of $Zn^{2+}$ which inhibits the corrosion of A3003 in model fresh water is 0.1 mM.

## Conclusions

The corrosion behavior and the corrosion products of A3003 alloy formed in fresh water containing different $Zn^{2+}$ concentration were investigated by immersion tests with AES observations and analysis.

1) The thickness of the corrosion product layer formed on A3003 decreases with increases in the $Zn^{2+}$ concentration of the model fresh water here.

2) Corrosion products formed on the A3003 in the solutions containing $Zn^{2+}$ ( > 0.1 mM) have a multi-layered structure.

3) The minimum concentration of $Zn^{2+}$ which can inhibit the corrosion of A3003 in the model fresh water here appears to be 0.1 mM.

4) The corrosion inhibition mechanism of $Zn^{2+}$ appears to be a two stage process. In the initial stage of immersion, $Zn^{2+}$ forms the metal cation layer on the $Al_2O_3$ and this layer suppresses the cathodic and anodic reactions on the A3003 alloy in the model fresh water. After long immersion, $Zn^{2+}$ and the dissolved $Al^{3+}$ form Zn/Al corrosion products and these products inhibit the cathodic reaction.

## Acknowledgments

This study was supported by the Salt Science Research Foundation (grant number 1609 and 1706) and The Light Metal Educational Foundation, Inc., and was conducted at Laboratory of XPS analysis, Hokkaido University, supported by “Nanotechnology Platform” Program of the Ministry of Education, Culture, Sports, Science and Technology (MEXT), Japan. This research was also supported by Japan Society for the Promotion of Science (JSPS) KAKENHI Grant Number 17J00602.

## References

1. Nguyen TH, Foley RT. The chemical nature of aluminum corrosion III . The dissolution

mechanism of aluminum oxide and aluminum powder in various electrolytes. J Electrochem Soc. 1980;127(12):2563-2566. https://doi.org/ 10.1149/1.2129520.

2. Foley RT. Localized corrosion of aluminum alloys — A Review. Corrosion. 1986;42(5):277-288. https://doi.org/10.5006/1.3584905

3. Zaid B, Saidi D, Benzaid A, Hadji S. Effects of pH and chloride concentration on pitting corrosion of AA6061 aluminum alloy. Corros Sci. 2008;50(7):1841-1847. https://doi.org/10.1016/j.corsci.2008.03.006

4. Editorial board of Japan Aluminium Association, Aluminum handbook. Tokyo: Japan Aluminium Association, 2007, 73.

5. Ito G, Ishida S, Kato M, Nakayama T, Mishima Y. The effect of minor impurities in water on corrosion of aluminum. Keikinzoku. 1968;18(10):530-536. https://doi.org/10.2464/jilm.18.530

6. Fujimura R, Koyama T, Uchida H. Influence of the cation species in $Cl^-$ containing solution on Corrosion of Al–Mg–Si Aloy. Keikinzoku. 2013;63(5):175-181. https://doi.org/10.2464/jilm.63.175.

7. Otani K, Sakairi M, Kikuchi T, Kaneko A. Effect of cations on corrosion behavior of aluminum alloy in model tap water. Zairyo-to-Kankyo. 2010;59(9):330-331. https://doi.org/10.3323/jcorr.59.330.

8. Sakairi M, Sasaki R, Kaneko A, Seki Y, Nagasawa D. Evaluation of metal cation effects on galvanic corrosion behavior of the A5052 aluminum alloy in low chloride ion containing solutions by electrochemical noise impedance. Electrochim Acta. 2014;131(10):123-129. https://doi.org/10.1016/j.electacta.2014.02.010.

9. Otani K, Sakairi M, Sasaki R, Kaneko A, Seki Y. Effect of metal cations on corrosion behavior and surface film structure of the A3003 aluminum alloy in model tap waters. J Solid State Electrochem. 2014;18(2):325-332. https://doi.org/10.1007/s10008-013-2260-7.

10. Otani K, Sakairi M, Kaneko A. Effect of a kind of metal cation on corrosion mechanism of A3003 aluminum alloy in tap water. Mater Trans. 2016;57(9):1539-1546. https://doi.org/10.2320/matertrans.M2016030.

11. Otani K, Sakairi M, Kaneko A, Nagasawa D. Corrosion-induced morphological changes and the mechanism of A3003 aluminum alloy in model sea water containing gluconates and zinc ions. Keikinzoku. 2018;68(1):16-21. https://doi.org/10.2464/jilm.68.16.

12. Alwitt RS. The growth of hydrous oxide films on aluminum. J Electrochem Soc. 1974;121(10):1322-1328. https://doi.org/10.1149/1.2401679

13. O'Grady WE, Roeper DF, Natishan PM. Structure of chlorine K-Edge XANES spectra during the breakdown of passive oxide films on aluminum. J Phys Chem. C. 2011;115(51): 25298-25303. https://doi.org/0.1021/jp2056305.

14. Natishana PM, O'Grady WE. Chloride ion interactions with oxide-covered aluminum leading to pitting corrosion: A Review. J Electrochem Soc. 2014;161(9):C421-C432. https://doi.org/10.1149/2.1011409jes.

15. Lewis GN. Valence and the structure of atoms and molecules, The Chemical Catalog Co. 1923.

16. Pearson RG. Hard and soft acids and bases. J Am Chem Soc. 1963;85(22):3533-3529.

17. Heydarpour MR, Zarrabi A, Attar MM, Ramezanzadeh B. Studying the corrosion protection properties of an epoxy coating containing different mixtures of strontium aluminum polyphosphate (SAPP) and zinc aluminum phosphate (ZPA) pigments. Prog Org Coat. 2014;77(1):160-167. https://doi.org/10.1016/j.porgcoat.2013.09.003.

18. Sanni O, Loto CA, Popoola API. Inhibitive behaviour of zinc gluconate on aluminium alloy in 3.5 % NaCl solution. Silicon. 2016;8(2):195-200. https://doi.org/10.1007/s12633-014-9180-8.

19. Ehsani A, Nasrollahzadeh M, Mahjani MG, Moshrefi R, Mostaanzadeh H. Electrochemical

and quantum chemical investigation of inhibitory of 1,4-Ph(OX)$_2$(Ts)$_2$ on corrosion of 1005 aluminum alloy in acidic medium. J Ind Eng Chem. 2014;20(6):4363-4370. https://doi.org/10.1016/j.jiec.2014.01.045.

20. Aramaki A. Inhibition effects of inorganic multivalent cations on iron corrosion in aerated sodium sulfate solution. Corrosion. 1998;55(2):157-165. https://doi.org/10.5006/1.3283976.

**Caption List**

Fig. 1 (a) Surface and (b) cross sectional SEM images of specimen before the immersion tests.

Fig. 2 Surface SEM images of specimens after immersion for 7 d (0.6 Ms) in (a) NaCl, (b) 0.01Zn, (c) 0.1Zn, and (d) 1.0Zn.

Fig. 3 Surface AES analysis of specimens after immersion for 7 d in model fresh water.

Fig. 4 Cross-sectional SEM images of specimens after immersion for 7 d in (a) NaCl, (b) 0.01Zn, (c) 0.1Zn, and (d) 1.0Zn.

Fig. 5 Cross-sectional AES point analysis of specimens after immersion for 7 d in (a) NaCl, (b) 0.01Zn, (c) 0.1Zn, and (d) 1.0Zn.

Fig. 6 Schematic representations of formation and corrosion protection mechanism of (a, b) metal cation layer of $Zn^{2+}$ and (c, d) Zn/Al corrosion products formed on the $Al_2O_3$ of the A3003 alloy in the model fresh water.

**Figures**

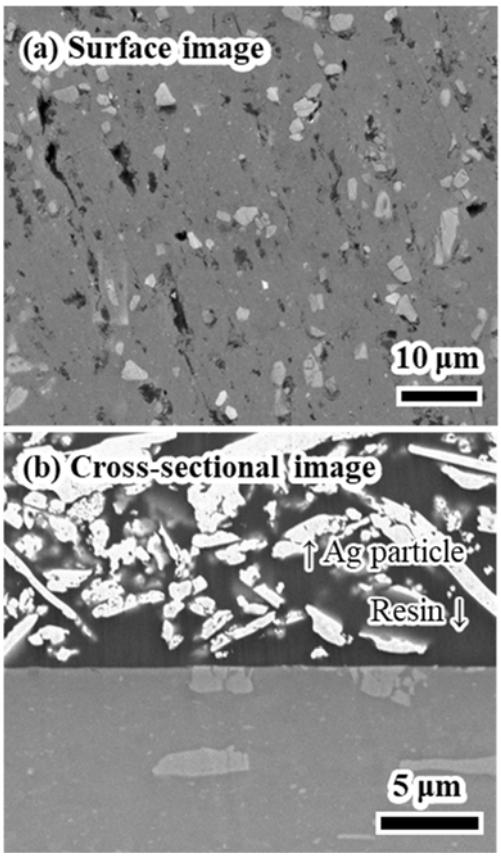


Fig. 1 (a) Surface and (b) cross sectional SEM images of specimens before the immersion tests.

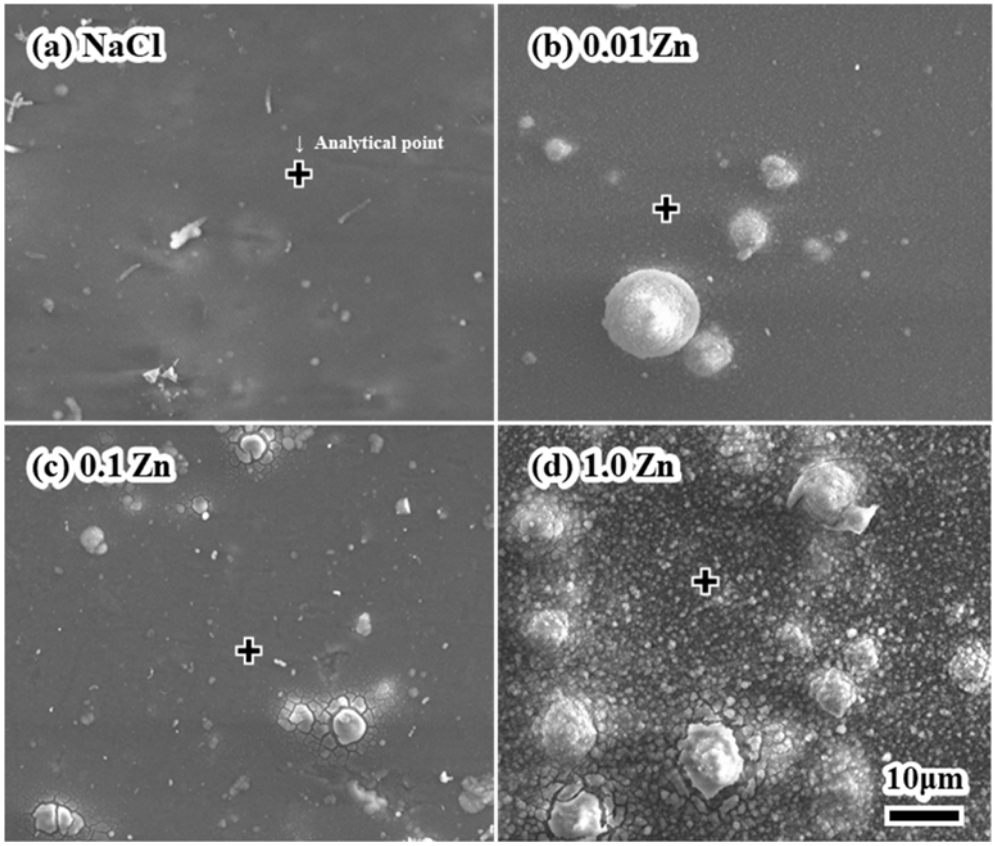


Fig. 2 Surface SEM images of specimens after immersion for 7 d (0.6 Ms) in (a) NaCl, (b) 0.01Zn, (c) 0.1Zn, and (d) 1.0Zn.

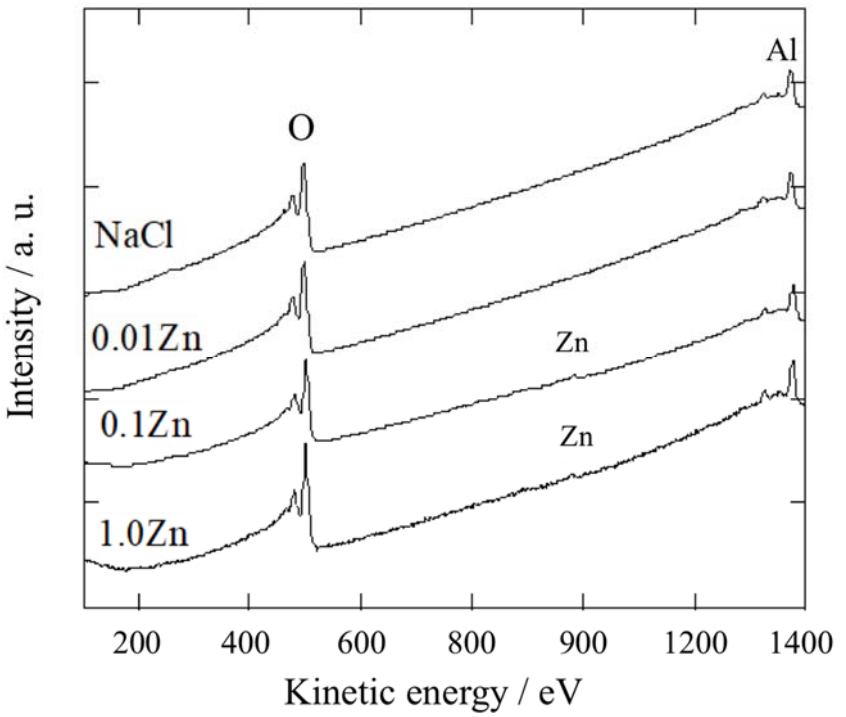


Fig. 3 Surface AES analysis of specimens after immersion for 7 d in model fresh water.

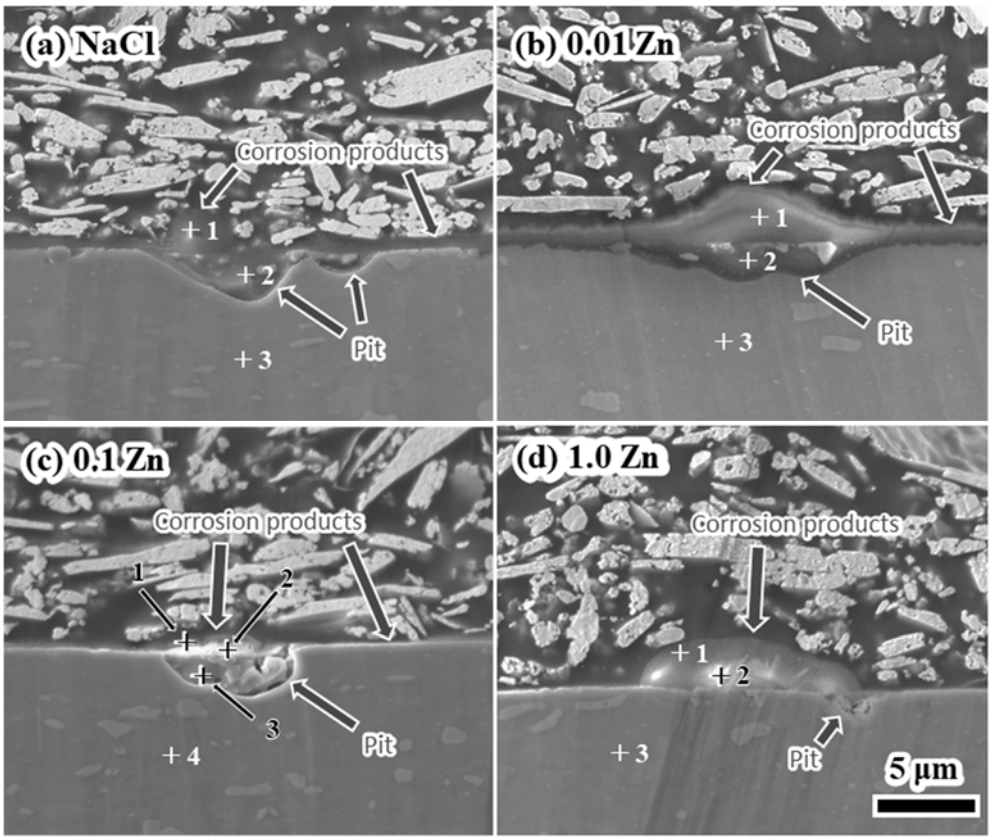


Fig. 4 Cross-sectional SEM images of specimens after immersion for 7 d in (a) NaCl, (b) 0.01Zn, (c) 0.1Zn, and (d) 1.0Zn.

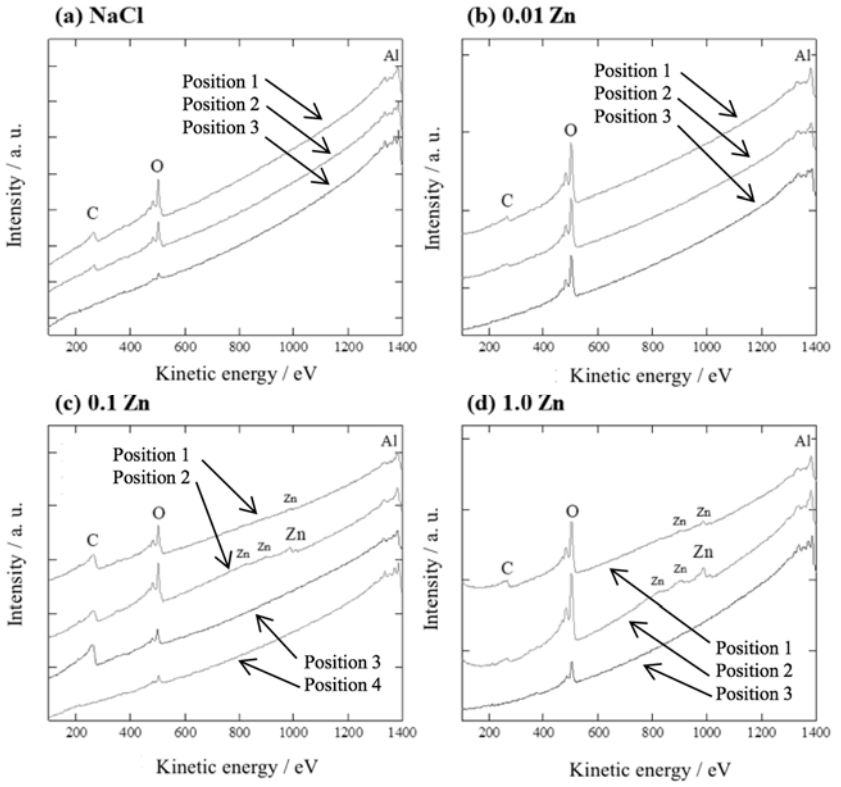


Fig. 5 Cross-sectional AES point analysis of specimens after immersion for 7 d in (a) NaCl, (b) 0.01Zn, (c) 0.1Zn, and (d) 1.0Zn.

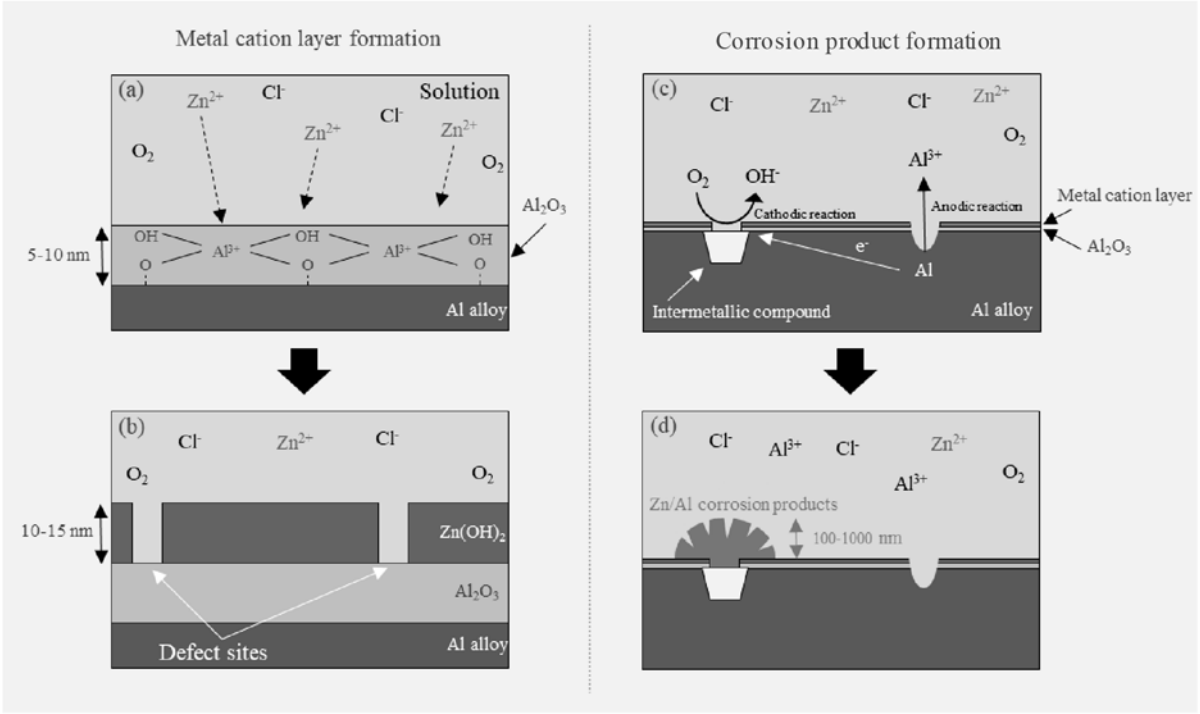


Fig. 6 Schematic representations of formation and corrosion protection mechanism of (a, b) metal cation layer of $Zn^{2+}$ and (c, d) Zn/Al corrosion products formed on the $Al_2O_3$ of the A3003 alloy in the model fresh water.